▐ Dyes

Unprecedented Strong Panchromic Absorption from Proton-Switchable Iridium(III) Azoimidazolate Complexes

Adam F. Henwood,[a] Yue Hu,[b] Muhammad T. Sajjad,[c] Gopala K. V. V. Thalluri,[c] Sanjay S. Ghosh,[c, d] David B. Cordes,[a] Alexandra M. Z. Slawin,[a] Ifor D. W. Samuel,[c] Neil Robertson,[b] and Eli Zysman-Colman*[a]

Abstract: Two new heteroleptic iridium(III) complexes bearing an aryldiazoimidazole ligand are reported. These complexes differ structurally with respect to the protonation state of the imidazole ring, but can be independently accessed by varying the synthetic conditions. Their structures have been unequivocally confirmed by X-ray crystal structure analysis, with surprising differences in the structural parameters of the two complexes. The strongly absorbing nature of the free diazoimidazole ligand is enhanced in these iridium complexes, with the protonated cationic complex demonstrating extraordinarily strong panchromic absorption up to 700 nm. The absorption profile of the deprotonated neutral complex is blueshifted by about 100 nm and thus the interconversion between the two complexes as a function of the acidity/basicity of the environment can be readily monitored by absorption spectroscopy. Theoretical calculations revealed the origins of these markedly different absorption properties. Finally, the protonated analogue has been targeted as an acceptor material for organic photovoltaic (OPV) applications, and preliminary results are reported.

Introduction

Aryldiazo moieties have attracted significant attention as an interesting class of ligand scaffold for metal complexes. Complexes employing such ligands often display broad absorption profiles, dominated by strong charge transfer (CT) bands,[1] as well as multiple reversible electrochemical reduction processes associated with the typically redox non-innocent nature of these ligands.[2] Exploitation of these optoelectronic properties

has led to reports of these materials being used as switches in optical recording media,[2a, 3] or as catalysts for small-molecule activation, in which multielectron processes play a crucial role.[4] Interest in such applications is magnified by the potential to utilize the dual coordination modes of the diazo moiety to construct multimetallic complexes that show enhanced CT properties or unique electrochemical behavior, such as mixed metal valency, which is also of use for catalytic applications.[1a, 5] Finally, significant efforts have been expended in grafting diazo units onto ligands of metal complexes that enable these complexes to act as photoswitches following the *cis/trans* isomerization of these units.[6]

Surprisingly, given the popularity of the use of these ligands with other metals, examples involving their complexation with iridium are scarce and can largely be divided into three main families. The first of these are the Ir^{I} complexes, such as **1**, in which the complexes are square planar and capped by a Cp* ligand (Scheme 1). A bidentate aryldiazo ligand and a monodentate ligand, such as water, fill the coordination sphere of these complexes.

Among Ir^{III} complexes, most examples resemble complex **2**, in which the diazo moiety is integral to a terdentate binding mode and is sandwiched by combinations of phenolate,[7] thiolate,[8] deprotonated aniline,[9] or cyclometalated carbanions.[7, 9] In this family of iridium complexes, the octahedral coordination sphere is completed by monodentate ligands, such as chloride, hydride, or phosphine. The final class of Ir^{III} complexes, exemplified by **3**, that involve the use of bidentate aryldiazo ligands possesses the smallest number of reported examples.[2a, 10]

Given our interest in the development of panchromatic iridium complexes[11] for solar-harvesting applications and the

[a] A. F. Henwood, Dr. D. B. Cordes, Prof. A. M. Z. Slawin, Dr. E. Zysman-Colman
Organic Semiconductor Centre, EaStCHEM School of Chemistry, University of St. Andrews, St. Andrews, Fife, KY16 9ST (UK)
Fax: (+44) 1334-463808
E-mail: eli.zysman-colman@st-andrews.ac.uk
Homepage: URL:http://www.zysman-colman.com

[b] Y. Hu, Prof. N. Robertson
EaStCHEM School of Chemistry, University of Edinburgh, King's Buildings, Edinburgh EH93FJ (UK)

[c] Dr. M. T. Sajjad, Dr. G. K. V. V. Thalluri, Dr. S. S. Ghosh, Prof. I. D. W. Samuel
Organic Semiconductor Centre, SUPA, School of Physics and Astronomy, University of St. Andrews, St. Andrews, Fife, KY16 9SS (UK)

[d] Dr. S. S. Ghosh
Current address: Optoelectronics Laboratory, Department of Physics, North Maharashtra University, Jalgaon-425001 (India)

⌨ Supporting information for this article is available on the WWW under http://dx.doi.org/10.1002/chem.201503546. The research data supporting this publication can be accessed at http://dx.doi.org/10.17630/4f97155a-1e28-42b2-a252-0846d4907010. CCDC 1401456 and 1401457 contain the supplementary crystallographic data for this paper. These data are provided free of charge by The Cambridge Crystallographic Data Centre.
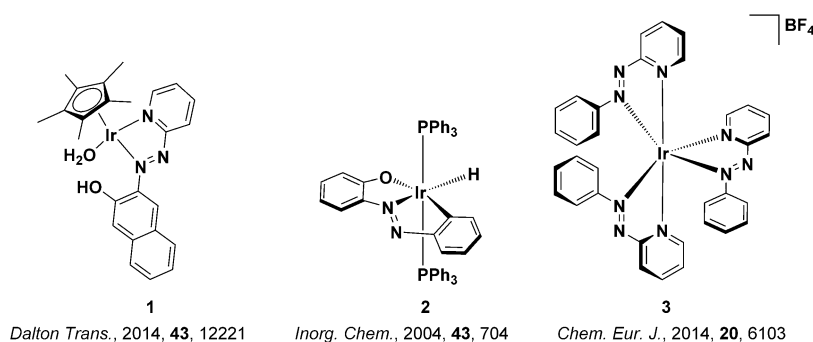
Scheme 1. Selected examples of iridium complexes bearing aryldiazo-type ligands.

promising optoelectronic properties of this class of ligand, we targeted complexes **4** and **5** for investigation. Notably, iridium (III) complexes typically demonstrate very poor absorption capabilities in the visible spectrum.[12] However, we recently reported that panchromatic iridium complexes are attainable using bis(iminoarylacenaphthene) (Ar-BIAN) ancillary ligands that contain donor aryl units linked to an acenaphthene acceptor core, thus promoting low-energy intraligand charge-transfer (ILCT) transitions.[11, 13] The most absorptive of this family of complexes employed a dimethylaniline donor, possessing an ILCT absorption band tailing off past 800 nm with a molar absorptivity of $7.1 \times 10^3 \, \text{M}^{-1} \text{cm}^{-1}$ at its λ_{max} at 675 nm.[13] Such an absorption profile is desirable for solar harvesting and is vastly superior to current state-of-the-art iridium dyes employed in solar cells, which show significant attenuation of their UV/Vis absorption profiles past 530 nm.[12g, 14]

Herein, we expand on our interests in panchromatic dyes by adopting the aryldiazo ligand 2-[4-(N,N-dimethylamino)-benzeneazo]imidazole (azoimH) as the ancillary ligand of two bis-cyclometalated iridium complexes also bearing 2-phenylpyridinato (ppy) cyclometalating ligands (**4** and **5** in Scheme 2). These complexes differ by the protonation state of the imidazole ring; both neutral and cationic complexes can be independently accessed through modulation of the complexation conditions.
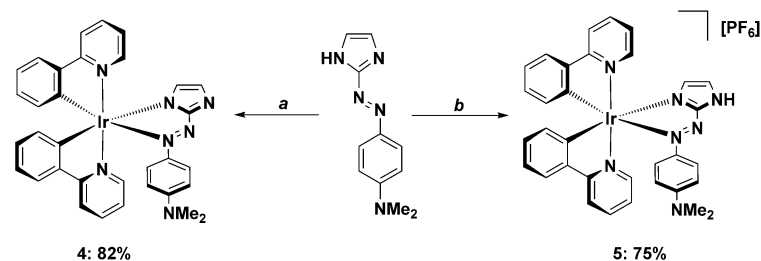
Results and Discussion

Synthesis

Cleavage of [Ir(ppy)₂(μ-Cl)]₂ dimer in the presence of excess K₂CO₃ gave neutral [Ir(ppy)₂(azoim)] (**4**) in excellent yield.[15] In the absence of base, [Ir(ppy)₂(azoimH)]⁺ (**5**) can be isolated as its PF₆ salt under standard conditions, also in high yield.[16] Remarkably, under these complexation conditions, the solution turned from red, which is the color of azoimH ligand, to a dark purple; under the basic conditions, described for the synthesis of **4**, the red color of the solution persisted, but noticeably darkened.

Solution-state structure analysis

The complex nature of the ¹H NMR spectra is indicative of the lowering of the symmetry about the iridium center following complexation (Figure 1). The ¹H NMR spectra for **4** and **5** showed similar features, particularly in the aromatic region. At higher frequency, multiplets at both approximately 8.05 and 7.75 ppm in **4** become more resolved in **5**. The distal NH proton in **5** could not be observed.

Solid-state structure analysis

Suitable crystals for X-ray diffraction analysis were obtained for both **4** and **5** (Figure 2). Selected geometric data is collected in Table 1. The X-ray structures support the absence/presence of the imidazoyl proton in these two respective complexes. The distal NH of **5** was located in the electron density map, positioned appropriately to form a hydrogen bond (1.77(2) Å) with a solvent water molecule. Surprisingly, changing the protonation state leads to a notable conformational change of the ancillary ligand. When the ligand is neutral, as in **5**, it is conformationally flat, but when deprotonated, as in **4**, a larger torsional twist (**4**: 33.6(6)°; **5**: −12.6(5)°) of the aryl ring with respect to the N-N-C-N azoimidazole plane is observed, which is coupled with a pyramidizilation and deconjugation of the NMe₂ group. This twisting

Scheme 2. Synthesis of **4** and **5**. Reagents and conditions: a) [Ir(ppy)₂(μ-Cl)]₂ (1.0 equiv), azoimH (2.2 equiv), K₂CO₃ (2.4 equiv), DCM/MeOH (5:4), 55 °C, 19 h. b) i) [Ir(ppy)₂(μ-Cl)]₂ (1.0 equiv), azoimH (2.5 equiv), DCM/MeOH (5:4), 55 °C, 19 h; ii) excess NH₄PF₆ (aq.).
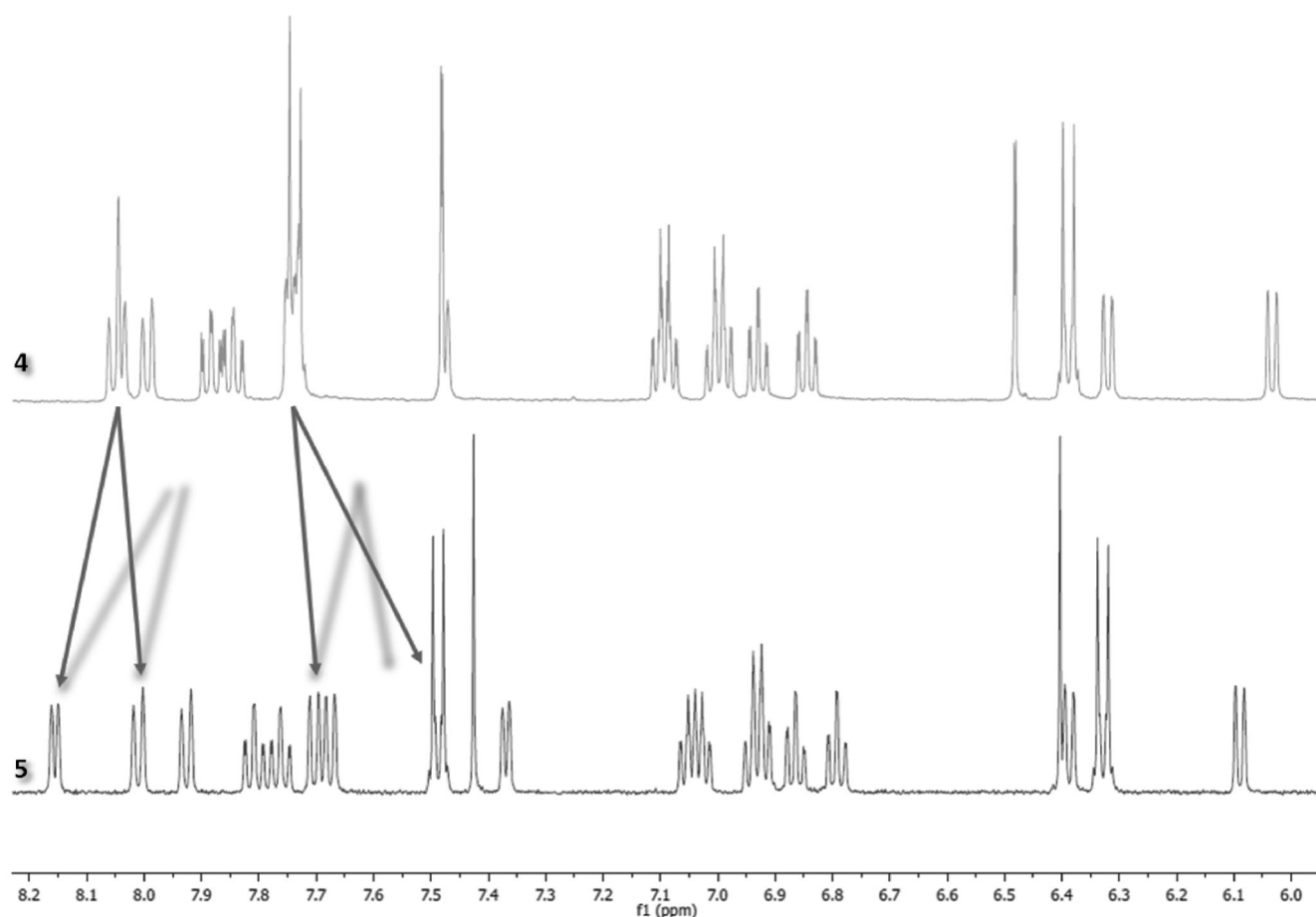
↖↖ **These are not the final page numbers!**

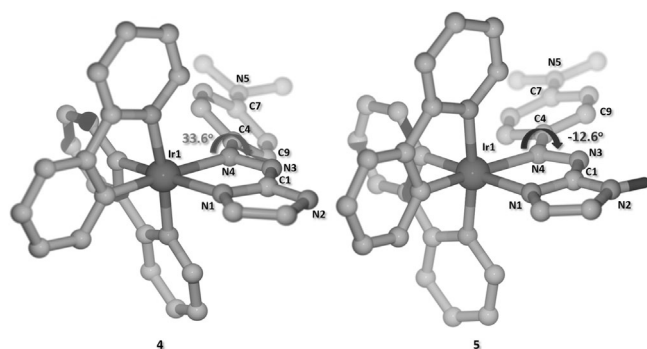**Figure 1.** Stacked aromatic region of the ^{1}H NMR spectra of **4** (top) and **5** (bottom) in CD$_3$CN at room temperature.

Figure 2. X-ray crystal structures of **4** (left) and **5** (right), annotated with N(3)-N(4)-C(4)-C(9) dihedral angles. Solvent molecules, counterions, and C—H hydrogen atoms are omitted for clarity.

Table 1. Selected bond lengths [Å] and angles [°], and torsion angles [°] for **4** and **5**.

4 [Ir(ppy)$_2$(azoim)]		**5** [Ir(ppy)$_2$(azoimH)](PF$_6$)	
Ir(1)—N(1)	2.110(4)	Ir(1)—N(1)	2.096(4)
Ir(1)—N(4)	2.167(4)	Ir(1)—N(4)	2.215(3)
N(1)—C(1)	1.364(6)	N(1)—C(1)	1.326(5)
N(2)—C(1)	1.355(6)	N(2)—C(1)	1.334(5)
N(3)—C(1)	1.359(6)	N(3)—C(1)	1.369(5)
N(3)—N(4)	1.297(5)	N(3)—N(4)	1.293(5)
N(4)—C(4)	1.416(6)	N(4)—C(4)	1.404(5)
N(5)—C(7)	1.385(6)	N(5)—C(7)	1.348(6)
N(1)-Ir(1)-N(4)	74.57(14)	N(1)-Ir(1)-N(4)	74.20(13)
N(1)-C(1)-N(2)	113.8(4)	N(1)-C(1)-N(2)	111.4(4)
N(3)-N(4)-C(4)	114.0(4)	N(3)-N(4)-C(4)	112.4(3)
N(3)-N(4)-C(4)-C(9)	33.7(6)	N(3)-N(4)-C(4)-C(9)	−12.6(5)

about the azoimidazole–aminophenyl bond is not significantly reflected in the N$_{azo}$—C$_{Ph}$ distances (**4**: 1.416(6) Å, **5**: 1.404(5) Å), but is more apparent for the deconjugation of the NMe$_2$ group, for which significant lengthening of the C$_{Ph}$—N$_{amine}$ distances is observed for **4** (**4**: 1.385(6) Å, **5**: 1.348(6) Å). The reduced conjugation within the ancillary ligand observed in the solid state for **4** may account for the blueshifted absorption
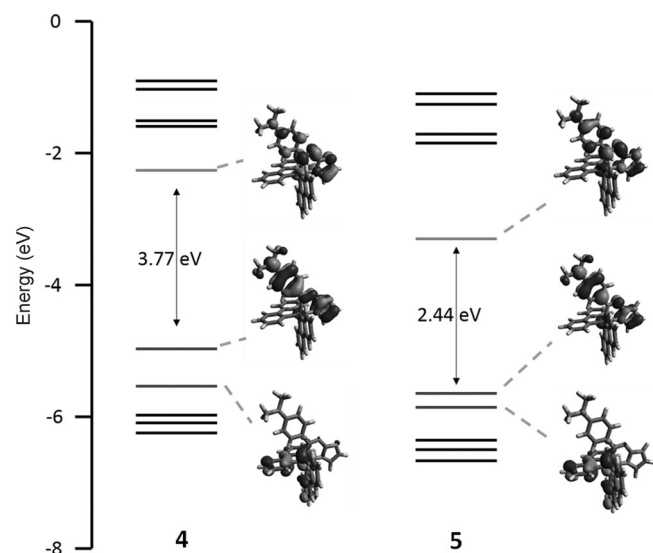
profile of **4** compared with **5** in solution and the solid state (see below).

Optoelectronic characterization and analysis

This electronic structure of the complexes was probed by DFT calculations, details of which can be found in the Supporting

These are not the final page numbers! ↗↗

Information. The solid-state trends regarding the N-*N*-C-N dihedral were generally supported by theory, with **4** retaining a slightly larger torsional twist than **5**, although smaller absolute dihedral angles were observed (5° for **4** and 3.4° for **5**; Table S2 in the Supporting Information).

The relevant relative orbital energies of **4** and **5** and their electronic distribution character are given in Figure 3 and
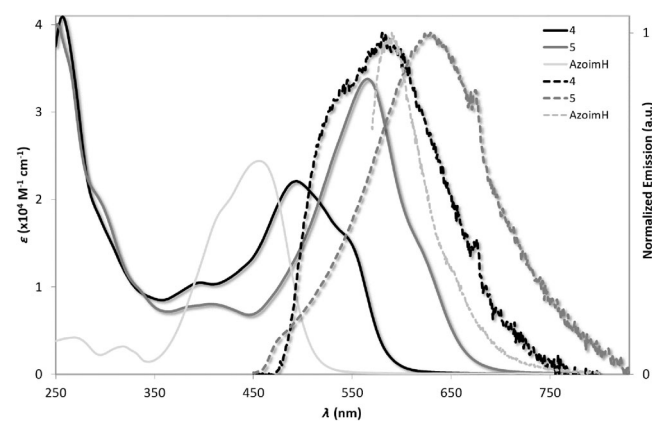
undergoes greater stabilization than the HOMO, providing an explanation for the greatly redshifted absorption spectrum seen for **5** compared to **4** (see below).

In the context of our initial observations of the color of the reaction solutions, we investigated the optoelectronic properties of **4** and **5** and contrasted these to the azoimH ligand. Figure 4 and Table 2 summarize the relevant data. Upon com-

Figure 3. Energy-level schemes for the Kohn–Sham orbitals of **4** and **5**, including selected Kohn–Sham orbitals and the HOMO–LUMO energy gap.

Figure 4. Absorption (solid lines) and normalized photoluminescence spectra (dashed lines) of the ligand azoimH in dichloromethane and **4** and **5** in MeCN.

Tables S3 and S4 in the Supporting Information. For both complexes, the HOMO is delocalized across the azoim(H) ligand, with the strongest contributions arising from the dimethylaniline fragment. The LUMO is also delocalized along the azoim(H) ligand, but resides most significantly on the imidazole fragment. Finally, the HOMO−1 for both complexes is primarily localized on the Ir atom, and the phenyl moiety of the ppy ligands; a pattern typically observed in the HOMO of most $[Ir(C^\wedge N)(N^\wedge N)]^+$-type complexes. Although both the HOMO and LUMO of **5** are stabilized upon protonation, the LUMO

plexation, the absorption profiles of **4** and **5** differ markedly from the parent ligand, particularly in the higher energy regimes: firstly, we observed very intense high-energy absorptions for both **4** and **5**, which are largely absent for the ligand, but are typical of many bis-cyclometalated iridium complexes.[16a, 17] Below 350 nm, these transitions are assigned to spin-allowed π–π* ligand-centered (^{1}LC) transitions localized on the ppy ligands, whereas between 350–450 nm, mixed metal-to-ligand charge-transfer (^{1}MLCT) and ligand-to-ligand charge-transfer (^{1}LLCT) absorptions to the azoimidazole ligand are operative.[17, 18] We noted also the increased absorptivity for **4** in this region, which is distinct from what was observed at lower energies.

Table 2. Relevant optoelectronic parameters for **4** and **5** at 298 K.[a]		
	4 [Ir(ppy)$_2$(azoim)]	**5** [Ir(ppy)$_2$(azoimH)][PF$_6$]
λ_{abs} [nm] [ε ($\times 10^4$/M^{-1} cm^{-1})]	256 [4.08], 304 sh [1.55], 392 [1.04], 493 [2.21], 546 sh [1.55]	252 [4.00], 297 sh [1.98], 406 [0.80], 565 [3.38], 616 sh [1.50]
λ_{em} [nm][b]	580	625
Φ_{PL} [%][b,c]	0.03	0.08
τ_e [ns][d]	4.82 (11%), 163 (19%), 1403 (69%)	108.7 (22%), 1215 (78%)
τ_e aerated [ns][d]	0.405 (19%), 4.57 (41%), 45.2 (40%)	8.46 (15%), 31.5 (85%)
$E^{ox}_{1/2}$ [V]	0.19	0.62
$E^{red}_{1/2}$ [V]	−1.82	−1.03
E_{HOMO} [eV][e]	−4.99	−5.42
E_{LUMO} [eV][f]	−2.98	−3.77
[a] Measurements were carried out in degassed MeCN, except for UV/Vis absorption and aerated lifetimes, which were conducted under air. Electrochemical measurements were performed at 100 mVs^{-1}, using Fc/Fc$^+$ as an internal standard and are referenced to the Fc/Fc$^+$ redox couple. [b] $\lambda_{exc} = 360$ nm. [c] Quinine sulfate was used as the reference ($\Phi_{PL} = 54.6$% in 0.5 M H$_2$SO$_4$ at 298 K).[19] [d] $\lambda_{exc} = 375$ nm. [e] $E_{HOMO} = -[E^{ox}_{vs.Fc/Fc+} + 4.8]$ eV. [f] $E_{LUMO} = -[E^{red}_{pa vs.Fc/Fc+} + 4.8]$ eV.[20]		

↖↖ **These are not the final page numbers!**

At low energies, the form of the absorption spectra for both the free ligand and the complexes are more similar, albeit with pronounced changes in the absolute energies at which these transitions occur. For the ligand, an intense shoulder (415 nm) and fully resolved band (458 nm) were observed. These bands are ascribed as CT transitions between the NMe_2 donor and the azoimidazole acceptor. Given the similar profiles, the same ILCT-type transitions are presumed to be operative within the complex framework as well, but with significant redshifting and enhancing of intensity of the transitions for the complexes compared with the free ligand. These low-energy absorptions (up to 700 nm for **5**) and unprecedentedly high extinction coefficients are in stark contrast to the absorption profiles of the vast majority of bis-cyclometalated iridium(III) complexes previously reported.[21] In compound **4**, this band peaks at 493 nm ($2.21 \times 10^4 \, M^{-1} cm^{-1}$), with a shoulder at 546 nm also observed. With complex **5**, protonation caused to redshift these bands by 72 nm ($2585 \, cm^{-1}$), with the principal band (565 nm) remarkably intense at $3.38 \times 10^4 \, M^{-1} cm^{-1}$. The high intensity observed for the shoulder at 616 nm for **5** ($1.50 \times 10^4 \, M^{-1} cm^{-1}$) compares favorably with our prior best absorbing aryl-BIAN-containing iridium complex, which exhibited an albeit redshifted ILCT absorption ($\lambda_{max} = 675$ nm) but at much lower molar absorptivity ($0.71 \times 10^4 \, M^{-1} cm^{-1}$).[11b]

The similar profiles of the absorption spectra suggest that the nature of the transitions occurring for both complexes (as well as the ligand) are fundamentally the same; these transitions were found at higher energy when the imidazole ring is formally anionic as in **4**. This implies that the trend in relative conformations seen in the solid state is also somewhat mirrored in solution with the reduced conjugation in **4** responsible for both the blueshifted absorption and the lower absorptivity compared to **5** (Figure 2). This trend is generally supported by theory, albeit with smaller calculated torsional angles for both complexes and a low barrier to rotation of the N-*N*-C-N torsion in MeCN solution (Table S2 in the Supporting Information).

To assess the nature of these transitions, time-dependent (TD) DFT calculations were performed, details of which can be found in in the Supporting Information. In compound **4**, the lowest-energy singlet electronic state arises from a HOMO→LUMO ILCT transition from the donor $ArNMe_2$ moiety to the azoimidazole acceptor. In compound **5**, the first two lowest-energy states are characterized by transitions arising from a combination of HOMO−1→LUMO and HOMO→LUMO. Their nature corresponds to an admixture of a similar ILCT-type transition observed for **4**, as well as MLCT contributions (Tables S5 and S6 in the Supporting Information). The simulated absorption profiles generally reproduce the trends observed experimentally, with **5** redshifted compared to **4**, but the overall spectra were predicted to be more blueshifted than experimentally observed (Figure 5).

UV/Vis absorption titration experiments revealed the reversibility of de/protonating the imidazole ring, and illustrate the large differences in energy of the lowest energy absorption bands between **4** and **5** ($2585 \, cm^{-1}$, 72 nm; Figure 6). Such energy differences are uncommon among proton-switchable
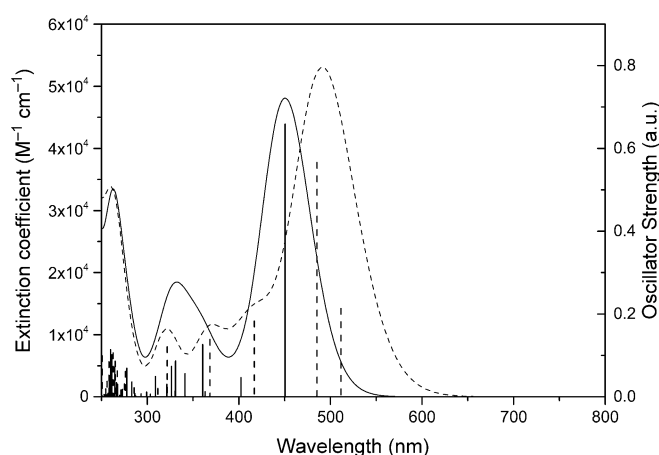

Figure 5. Simulated absorption spectra with oscillator strength (vertical lines) for **4** (——) and **5** (- - - -) by using CAM-B3LYP functional.
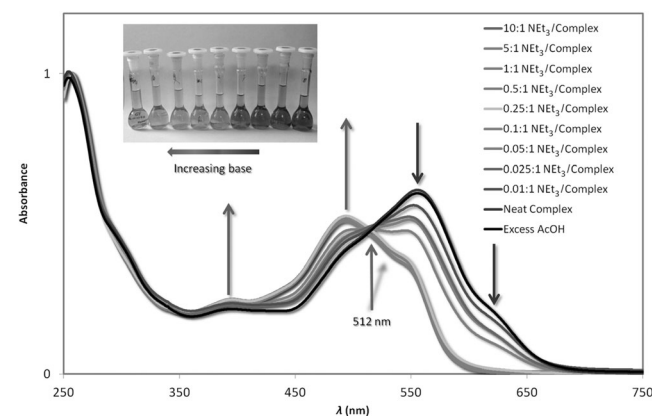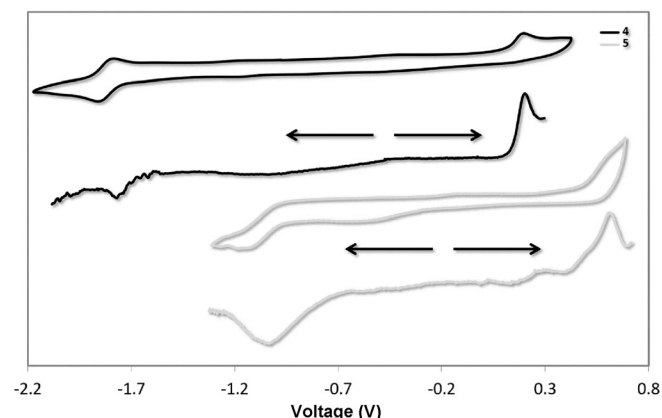

Figure 6. UV/Vis absorption titration, showing addition of varying equivalents of NEt_3 to a solution of **5** in MeCN. The spectra are normalized to the band at 257 nm. A curve showing **5** with addition of excess AcOH is shown for reference, overlapping exactly with the spectrum of the neat complex. Inset is an image of the titrated solutions, changing from deep purple to pink red upon addition of base.

iridium complexes. For example, Wenger's $[Ir(tolpy)_2(H_2biim)]$ $[PF_6]$ complex undergoes only a modest $498 \, cm^{-1}$ (12 nm) bathochromic shift in the emission energy upon monodeprotonation of the H_2biim ancillary ligand (tolpyH = 2-(4-methylphenyl)pyridine; H_2biim = 1,1′-biimidazole).[22] Williams and co-workers reported a switchable iridium complex bearing a 2-pyridylbenzimidazole ancillary ligand, in which the protonated form emits $3212 \, cm^{-1}$ (94 nm) lower in energy (496 nm neutral, 590 nm charged).[15a] Finally, Aoki and co-workers have reported significant stabilization in energy for their tris-cyclometalated iridium complex bearing an acid-responsive 4-pyridyl group (57 nm, $4223 \, cm^{-1}$ for absorption and 87 nm, $2899 \, cm^{-1}$ for emission).[23] However, in this example, the pyridyl groups are appended to the cyclometalated phenyl rings, which are typically associated with the HOMO of these complexes, pointing towards HOMO modulation rather than the LUMO modulation observed in our system.

Emission spectroscopy data revealed more insight into the excited state properties of these complexes. The ligand itself is poorly emissive, with a fluorescence signal detected at 592 nm. Similarly, the complexes are also poorly emissive ($\Phi_{PL} < 0.1\%$), which is typical for many metal–azo complexes.[10a] The multiexponential decay kinetics observed point towards significant quenching processes deactivating the excited state. Indeed, such behavior has been studied[1b] with an analogous ruthenium complex [Ru(bpy)$_2$(pap)](ClO$_4$)$_2$ (bpy = 2,2′-bipyridine; pap = 2-(phenylazo)pyridine). The totally non-emissive nature of this complex is attributed to a combination of conventional energy gap law vibrational quenching due to the redshifted absorption imparted by the azo ligand, as well as to sequential population of the ^{1}MLCT→^{3}MLCT$_{bpy}$→^{3}MLCT$_{pap}$ excited states, in which eventual de-excitation of the ^{3}MLCT$_{pap}$ state occurs non-radiatively within 4.5 ns. In an analogous fashion, it is possible that 4 and 5 undergo a similar process (^{1}MLCT→^{3}MLCT$_{ppy}$→^{3}MLCT$_{azoim(H)}$). However, in these examples, energy transfer from the ^{3}MLCT$_{ppy}$ state to the ^{3}MLCT$_{azoim(H)}$ state is not as efficient as the ruthenium analogue reported by Ghosh and Palit, giving rise to a long-lived phosphorescent component from the ^{3}MLCT$_{ppy}$ state.[1b] Such excited-state dynamics would account for the peculiarly small Stokes shifts observed for these complexes (45 nm or 1419 cm^{-1} for 4 and 14 nm or 361 cm^{-1} for 5). Under aerated conditions, this emission is quenched significantly, which further points to population of a long-lived triplet excited state.

Electrochemistry

Cyclic (CV) and differential pulse voltammetry (DPV) measurements were undertaken to discern the energy levels of these materials (Figure 7 and Table 2). The oxidation processes are uncharacteristic of typical bis-cyclometalated iridium(III) complexes. For example, [Ir(ppy)$_2$(bpy)]PF$_6$ possesses a pseudo-reversible first oxidation wave at 0.89 V (vs. Fc/Fc$^+$) that has been attributed to the Ir^{III}/Ir^{IV} redox couple along with contribution from the phenyl moieties of the cyclo-

metalating ligands.[24] By comparison, here the oxidation waves are at much less positive potential (0.19 V for 4 and 0.62 for 5, vs. Fc/Fc$^+$) and are completely irreversible. This suggests that the oxidation process is purely ligand-centered. The changes in the electrochemistry as a function of the protonation state of the ancillary ligand can be rationalized as a function of the charge of the complex. When protonated, the complex is +1 charged, and thus a single-electron oxidation of 5 would generate a formal +2 cation. This is thermodynamically more difficult than the analogous process of generating a formal +1 cation in the oxidation of 4, which explains the moderately greater anodic potential observed for 5. The same arguments hold for the reduction: The positive charge on 5 makes for facile reduction (−1.03 vs. Fc/Fc$^+$) to the charge-neutral species compared with reduction of the formally neutral 4 to a radical anion, which occurs at substantially more negative potential (−1.82 vs. Fc/Fc$^+$). The ligand-centered assignment of the electrochemistry, as well as the thermodynamic arguments, are in general agreement with energy changes predicted by the DFT calculations (see above).

OPV devices

The panchromic absorption properties of 5 make it an interesting candidate for solar-cell applications. To assess this suitability further, a photophysical study of this complex in thin films was carried out, with a view to employing this material in solution-processed organic photovoltaics (OPV). Initial spin-coated films from neat solutions of 5 were of poor quality, which lead us to explore blending it with a polymer. Given the strong stabilization of both the HOMO and LUMO of 5, it was anticipated that this material might function as an acceptor material in an OPV device. Poly(3-hexylthiophen-2,5-diyl) (P3HT) was chosen as the donor material. Films of P3HT/5 in a 1:0.5 ratio were studied. The similar absorption spectra of a neat film of P3HT and a blend are shown in Figure 8. The blend demonstrates good overlap with the neat film but has more pronounced vibronic features, leading to slightly more absorption at longer wavelengths.
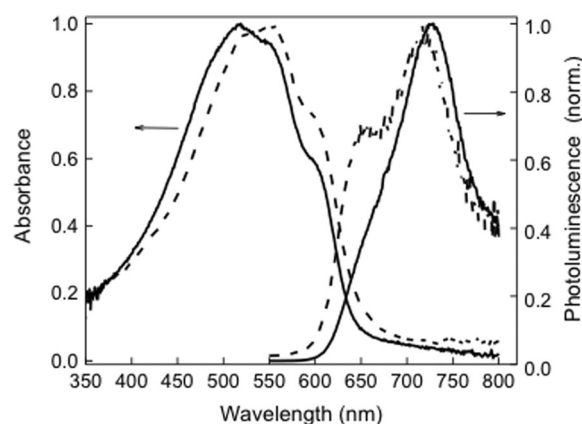

Figure 7. Cyclic and differential pulse voltammetry measurements showing first oxidation and reduction potentials of complexes 4 and 5 in MeCN, referenced vs Fc/Fc$^+$. Scan rate: 100 mV s^{-1}. Arrows indicate DPV scan directions.

Figure 8. Absorption and PL spectra of pristine P3HT (——) and P3HT/5 (1:0.5) (-----) films on quartz substrates. PL spectra were collected after excitation at 400 nm.

↖↖ These are not the final page numbers!

A necessary condition for efficient charge generation in the OPV device is that there should be efficient PL quenching of the donor. Accordingly, we investigated photoluminescence quenching using both time-resolved photoluminescence (TRPL) and photoluminescence quantum yield (Φ_{PL}) measurements of the blend (P3HT/**5**), and compared these with the pristine P3HT film. Figure 9 shows increased PL quenching for
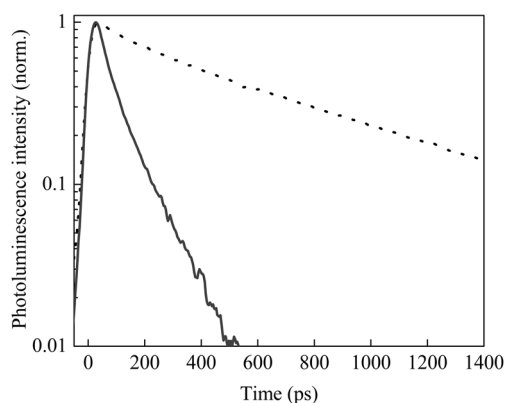
Figure 9. TRPL spectra of pristine P3HT (••••) and P3HT/**5** (——) films on quartz substrates. The films were excited at 400 nm and emission detected at 650 nm.

the blend compared to pristine P3HT—a lifetime (τ_e) of 603 ± 12 ps was measured for the pristine P3HT film, compared with just 75 ± 4 ps for the blend. To calculate the charge-transfer quenching efficiency (η_{et}), we integrated the entire decay of P3HT with and without complex **5** and used the differences in the area to calculate η_{et}, as shown in Equation (1):[25]

$$\eta_{et} = 1 - \frac{\int I(\text{P3HT with 5})dt}{\int I(\text{neat P3HT})dt} \qquad (1)$$

in which I(P3HT with **5**) and I(neat P3HT) are the intensity decays of P3HT with **5** and neat P3HT, respectively. A PL quenching efficiency of $80 \pm 6\%$ was obtained for the investigated blend (1:0.5) by using Equation (1).

For comparison, the quenching efficiency was also calculated from Φ_{PL} measurements. The measured Φ_{PL} of neat P3HT was found to be $8.8 \pm 0.3\%$, whereas Φ_{PL} of the blended film was $1.2 \pm 0.1\%$ (Table 2). The efficiency of quenching was calculated according to Equation (2):

$$\eta_{et} = 1 - \frac{\phi_{PL}(\text{P3HT with 5})}{\phi_{PL}(\text{neat P3HT})} \qquad (2)$$

The calculated quenching efficiency was $86 \pm 9\%$ for the blend. The estimates of quenching efficiency from TRPL and PLQY are similar and show that there is substantial, but not complete quenching. It is likely that quenching is due to both a combination of charge transfer and energy-transfer processes.

The device configuration is given in Figure 10, whereas the current/voltage (*I/V*) characteristics and device performance are shown in Figure 11. The most striking feature of the OPV performance is the exceptionally high open-circuit voltage (V_{oc}) of 1.12 V obtained from the blend (P3HT/**5**) compared to the
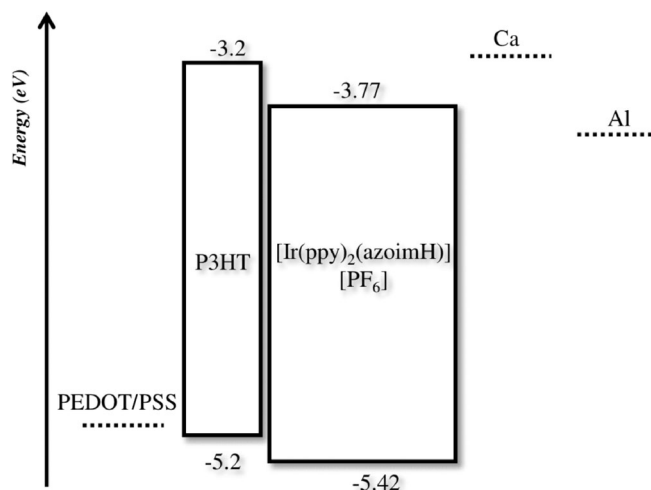
Figure 10. HOMO–LUMO energy-level band diagram of relevant materials employed in the OPV device.
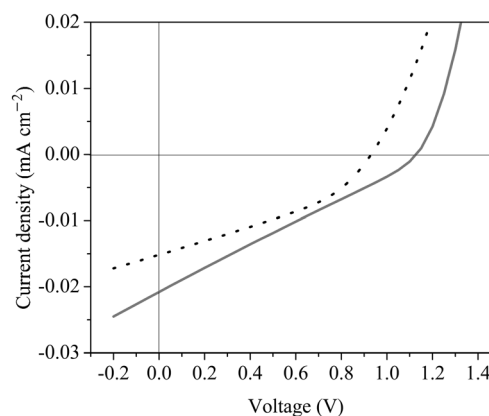
Figure 11. I/V characteristics for pristine P3HT (••••) and P3HT/**5** (——) bulk heterojunction solar cells.

device containing P3HT only (0.93 V). These V_{oc} values are higher than that reported for other solution-processed iridium complexes, which are in the range of 0.7 to 0.8 V.[12h, 26] This high V_{oc} can be understood from consideration of the energy levels, which are related by Equation (3):[27]

$$V_{oc} = \text{HOMO}_{\text{donor}} - \text{LUMO}_{\text{acceptor}} - 0.3 \qquad (3)$$

Equation (3) gives an estimated V_{oc} of 1.13 V, which is in good agreement with the experimentally determined value. Such a high observed V_{oc}, particularly compared with other iridium-based devices, is attributable to the device configuration, in which the iridium complex is acting as an acceptor, rather

than as a donor, as was the case in previous reports.[12g,h,26] The strongly stabilized HOMO and LUMO energy levels in **5** make this complex viable from a thermodynamic standpoint to function as an acceptor for the P3HT donor. By contrast, the anionic charge on the imidazolate moiety of **4** destabilizes the energy of the HOMO and LUMO to the extent that this is no longer possible.

Unfortunately, despite the high observed V_{oc} of the OPV device and efficient photoluminescence quenching of P3HT by **5**, the overall device performance is poor. In general, low short circuit currents can arise from inefficient charge separation, poor charge transport and leakage of the charge carriers to the electrodes. Although efficient quenching was observed, it is possible that there is considerable energy transfer from P3HT to **5**. In such instances, charge generation would be impaired, which perhaps provides an explanation why the device performance is poor. Such a problem could be overcome by designing materials that display even lower HOMO energy levels.

Conclusion

We have synthesized two new iridium complexes bearing azoimidazole/imidazolate ligands, and their photophysical properties were studied. Both complexes are strongly absorptive, with **5** in particular demonstrating absorption up to 700 nm, with very high molar extinction coefficients at long wavelengths $(1.50 \times 10^4 \, \text{M}^{-1} \, \text{cm}^{-1}$ at 616 nm). (De)protonation of the imidazole ring is fully reversible, and the energetic differences in the absorption profiles of **4** and **5** upon the addition of acid or base are unusually large, particularly compared to other iridium-based systems. The strong absorption observed for **5** led us to explore its use in OPV devices. Although a high V_{oc} value was obtained, the overall device performance was poor. Nevertheless, the first example of an iridium-based acceptor material is reported.

Acknowledgements

[1] a) S. Kohlmann, S. Ernst, W. Kaim, *Angew. Chem. Int. Ed. Engl.* **1985**, *24*, 684; *Angew. Chem.* **1985**, *97*, 698; b) R. Ghosh, D. K. Palit, *Phys. Chem. Chem. Phys.* **2014**, *16*, 219.

[2] a) S. Goswami, D. Sengupta, N. D. Paul, T. K. Mondal, S. Goswami, *Chem. Eur. J.* **2014**, *20*, 6103; b) S. Patra, B. Sarkar, S. Maji, J. Fiedler, F. A. Urbanos, R. Jimenez-Aparicio, W. Kaim, G. K. Lahiri, *Chem. Eur. J.* **2006**, *12*, 489; c) S. Roy, I. Hartenbach, B. Sarkar, *Eur. J. Inorg. Chem.* **2009**, *2009*, 2553.

[3] a) F. Huang, Y. Wu, D. Gu, F. Gan, *Thin Solid Films* **2005**, *483*, 251; b) F. Huang, Y. Wu, D. Gu, F. Gan, *Mater. Lett.* **2004**, *58*, 2461.

[4] a) W. B. Yu, Q. Y. He, H. T. Shi, Y. Pan, X. Wei, *Dalton Trans.* **2014**, *43*, 12221; b) G. Albertin, S. Antoniutti, M. Bortoluzzi, J. Castro-Fojo, S. Garcia-Fontán, *Inorg. Chem.* **2004**, *43*, 4511.

[5] W. Kaim, *Coord. Chem. Rev.* **2001**, *219–221*, 463.

[6] a) S. Kume, H. Nishihara, *Dalton Trans.* **2008**, 3260; b) T. Yutaka, I. Mori, M. Kurihara, J. Mizutani, N. Tamai, T. Kawai, M. Irie, H. Nishihara, *Inorg. Chem.* **2002**, *41*, 7143.

[7] a) S. Baksi, D. K. Seth, H. Tadesse, A. J. Blake, S. Bhattacharya, *J. Organomet. Chem.* **2010**, *695*, 1111; b) R. Acharyya, F. Basuli, R.-Z. Wang, T. C. W. Mak, S. Bhattacharya, *Inorg. Chem.* **2004**, *43*, 704.

[8] D. Sardar, P. Datta, P. Mitra, C. Sinha, *Polyhedron* **2010**, *29*, 3170.

[9] J. L. Pratihar, P. Pattanayak, D. Patra, R. Rathore, S. Chattopadhyay, *Inorg. Chim. Acta* **2011**, *367*, 182.

[10] a) M. Panda, N. D. Paul, S. Joy, C.-H. Hung, S. Goswami, *Inorg. Chim. Acta* **2011**, *372*, 168; b) M. Panda, C. Das, G. H. Lee, S. M. Peng, S. Goswami, *Dalton Trans.* **2004**, 2655; c) M. Shivakumar, J. Gangopadhyay, A. Chakravorty, *Polyhedron* **2001**, *20*, 2089; d) S. Frantz, R. Reinhardt, S. Greulich, M. Wanner, J. Fiedler, C. Duboc-Toia, W. Kaim, *Dalton Trans.* **2003**, 3370; e) W. Kaim, R. Reinhardt, S. Greulich, J. Fiedler, *Organometallics* **2003**, *22*, 2240.

[11] a) K. Hasan, E. Zysman-Colman, *J. Phys. Org. Chem.* **2012**, *26*, 274; b) K. Hasan, E. Zysman-Colman, *Eur. J. Inorg. Chem.* **2013**, *2013*, 4421.

[12] a) E. Baranoff, J.-H. Yum, M. Graetzel, M. K. Nazeeruddin, *J. Organomet. Chem.* **2009**, *694*, 2661; b) Z. Ning, Q. Zhang, W. Wu, H. Tian, *J. Organomet. Chem.* **2009**, *694*, 2705; c) D. Wang, H. Dong, Y. Wu, Y. Yu, G. Zhou, L. Li, Z. Wu, M. Gao, G. Wang, *J. Organomet. Chem.* **2015**, *775*, 55; d) D. Wang, Y. Wu, H. Dong, Z. Qin, D. Zhao, Y. Yu, G. Zhou, B. Jiao, Z. Wu, M. Gao, G. Wang, *Org. Electron.* **2013**, *14*, 3297; e) E. I. Mayo, K. Kilsa, T. Tirrell, P. I. Djurovich, A. Tamayo, M. E. Thompson, N. S. Lewis, H. B. Gray, *Photochem. Photobiol. Sci.* **2006**, *5*, 871; f) N. Wang, J. Yu, Y. Zheng, Z. Guan, Y. Jiang, *J. Phys. Chem. C* **2012**, *116*, 5887; g) T. B. Fleetham, Z. Wang, J. Li, *Inorg. Chem.* **2013**, *52*, 7338; h) H. Zhen, Q. Hou, K. Li, Z. Ma, S. Fabiano, F. Gao, F. Zhang, *J. Mater. Chem. A* **2014**, *2*, 12390.

[13] K. Hasan, E. Zysman-Colman, *J. Phys. Org. Chem.* **2013**, *26*, 274.

[14] E. Baranoff, J.-H. Yum, I. Jung, R. Vulcano, M. Grätzel, M. K. Nazeeruddin, *Chem. Asian J.* **2010**, *5*, 496.

[15] a) L. Murphy, A. Congreve, L. O. Palsson, J. A. G. Williams, *Chem. Commun.* **2010**, *46*, 8743; b) S. Ladouceur, L. Donato, M. Romain, B. P. Mudraboyina, M. B. Johansen, J. A. Wisner, E. Zysman-Colman, *Dalton Trans.* **2013**, *42*, 8838.

[16] a) S. Ladouceur, E. Zysman-Colman, *Eur. J. Inorg. Chem.* **2013**, *2013*, 2985; b) M. Nonoyama, *Bull. Chem. Soc. Jpn.* **1974**, *47*, 767.

[17] L. Flamigni, A. Barbieri, C. Sabatini, B. Ventura, F. Barigelletti, *Top. Curr. Chem.* **2007**, *281*, 143.

[18] S. Ladouceur, D. Fortin, E. Zysman-Colman, *Inorg. Chem.* **2010**, *49*, 5625.

[19] W. H. Melhuish, *J. Phys. Chem.* **1961**, *65*, 229.

[20] C. M. Cardona, W. Li, A. E. Kaifer, D. Stockdale, G. C. Bazan, *Adv. Mater.* **2011**, *23*, 2367.

[21] Y. You, W. Nam, *Chem. Soc. Rev.* **2012**, *41*, 7061.

[22] J. C. Freys, G. Bernardinelli, O. S. Wenger, *Chem. Commun.* **2008**, 4267.

[23] A. Nakagawa, Y. Hisamatsu, S. Moromizato, M. Kohno, S. Aoki, *Inorg. Chem.* **2014**, *53*, 409.

[24] S. Ladouceur, D. Fortin, E. Zysman-Colman, *Inorg. Chem.* **2011**, *50*, 11514.

[25] J. R. Lakowicz, *Principles of fluorescence spectroscopy*, 3rd ed., Springer, **2006**.

[26] M. Qian, R. Zhang, J. Hao, W. Zhang, Q. Zhang, J. Wang, Y. Tao, S. Chen, J. Fang, W. Huang, *Adv. Mater.* **2015**, *27*, 3546.

[27] M. C. Scharber, D. Mühlbacher, M. Koppe, P. Denk, C. Waldauf, A. J. Heeger, C. J. Brabec, *Adv. Mater.* **2006**, *18*, 789.

FULL PAPER

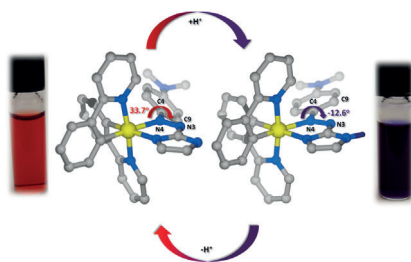**Organic photovoltaic applications**: Two new iridium complexes containing azoimidazole/imidazolate ligands were synthesized, and their photophysical properties were studied. Both complexes are strongly absorptive, demonstrating absorption up to 700 nm, with very high molar extinction coefficients at long wavelengths (see scheme).

Dyes

A. F. Henwood, Y. Hu, M. T. Sajjad,
G. K. V. V. Thalluri, S. S. Ghosh,
D. B. Cordes, A. M. Z. Slawin,
I. D. W. Samuel, N. Robertson,
E. Zysman-Colman*

■■ – ■■

Unprecedented Strong Panchromic Absorption from Proton-Switchable Iridium(III) Azoimidazolate Complexes

These are not the final page numbers! ↗↗